

Synthesis, Characterization and *In Vitro* Antibacterial Effect of 4*H*-Benzo[*g*]chromene Derivatives using Nano-NiO

T. CLARINA, G. R. PRIYA DHARSINI and V. RAMA*

Department of Chemistry, Sarah Tucker College, Manonmaniam Sundarnar University,
Abishekapatti, Tirunelveli -627 012, Tamilnadu, India

rama242002@gmail.com

Received 26 June 2017 / Accepted 20 July 2017

Abstract: The domino Knoevenagel cyclocondensation reactions *via* substituted aldehydes, activated methylene reagent and 2-hydroxy-1, 4-naphthoquinone gives benzo[*g*]chromenes in presence of nano-NiO using acetonitrile as a solvent at ambient temperature. This method gives the desired products from good to excellent yield. The salient features of this atom economical procedure are ease of manipulation, simpler workup, high yield processing, easy handling, inexpensiveness, reusability of catalyst and tolerance to a wide range of functional groups. The synthesized chromene derivatives are screened for antibacterial activity and antifungal activity using Kirby-Bauer method. The synthesized compounds **3a-3k** exhibits significant inhibition to antibacterial and antifungal activity compared with the standard drug Ciprofloxacin and Flucanazole respectively.

Keywords: Antibacterial, Knoevenagel condensation, Michael cyclization, Nano-NiO, Simple workup

Introduction

Chromene is a heterocyclic compound which contains benzene ring fused to a pyran ring. It is one of the privileged scaffolds with a medicinal pharmacophore such as antivasular, antimicrobial, antioxidant, anticoagulant, estrogenic, anti-helminthic, anticancer¹, anti-HIV, anti-inflammatory², analgesic, herbicidal³ and anticonvulsant. Chromenes are an important natural occurring compound such as flavonoids, alkaloids, tocopherol and anthocyanin⁴⁻⁶. Benzo[*g*]chromene contains naphthoquinone structural motifs which also have a broad spectrum in biological activities, as molecular probes for biochemical research⁷, emitters in electroluminescence devices and as fluorescent whitening agents⁸. The conventional method for the synthesis of chromene derivatives were found to have many drawbacks such as less effectiveness, low yield, formation of intermediates and long reaction time. To overcome these drawbacks, MCR was found to be suitable method for the synthesis of the compound without isolation of the intermediates and within a short reaction time. This method was

underwent by using various catalyst such as TEBA⁹, Et₃N¹⁰, DBU¹¹, Ionic liquids¹², Zn (*L*-Proline)₂¹³, POPINO¹⁴, Urea¹⁵ and OBS¹⁶. However, these methods suffer from certain drawbacks such as long reaction time, high temperature, toxic solvent, homogeneous catalyst, tedious workup and high catalyst loading. To avoid these drawbacks, it is in need of more efficient process for the synthesis of benzo[*g*]chromenes.

In continuation of our efforts, we report a simple, efficient synthesis of benzo[*g*]chromenes using reusable heterogeneous solid transition metal oxide nanoparticles as a catalyst. This transition metal nanoparticles shows a great attention in many scientific and technological fields including catalysis¹⁷. Their performances are good in selectivity, reactivity and yield of products due to high surface area and low coordinating sites. The surface area is high due to small particle size which is responsible for catalytic activity to enhance the yield of products. To the best of our knowledge there is no report available in the literature using nano-NiO as catalyst for the synthesis of benzo[*g*]chromenes in presence of acetonitrile as solvent.

Experimental

Transmission electron microscopy images were obtained on a Jeol/JEM 2100 TEM instrument with voltage 200 KV. The SEM Images were studied using a Jeol 7401F instrument. The XRD pattern of the catalyst samples was measured using a Cu K α radiation, $K = 1.54056 \text{ \AA}$ and operating condition of 40 kV and 30 mA in the 2θ range 10-80° at the scan speed of 0.05° per second. All ¹H NMR spectra were recorded on Bruker 400 MHz spectrometer in CDCl₃ and DMSO-*d*₆ with TMS as the internal standard. Inductively coupled plasma (ICP) was carried out on thermo electron IRIS intrepid II XSP DUO. The percentage of elements C, H and N in an organic compound are analyzed by using the instrument elemental vario EL III over a wide range of sample matrices and concentration. FTIR spectra were recorded on Shimadzu FT-IR 8400S using KBr pellets with the scanning range of 4000-400 cm⁻¹ and the resolution was 4 cm⁻¹. Melting points of isolated products were measured by using the open capillary method. The products synthesized were known compounds, confirmed by melting points and characterized by FT-IR and NMR spectroscopy.

General procedure for the preparation of nano-NiO

Nano-NiO was synthesized by the sol-gel reaction. Nano-NiO preparation was carried out by drop wise slow addition of 0.1 M sodium hydroxide (NaOH) to 0.1 M nickel nitrate, Ni(NO₃)₂·6H₂O with vigorous stirring of the solution continued until the pH reached 7.2. The mixed solution was stirred by magnetic stirring apparatus (1000 rpm) at room temperature. The resultant light-green precipitate was filtered and then washed with deionized water and ethanol for 5-10 times and was dried in an air oven for overnight, then calcined in muffle furnace at 450 °C for 3 hours.

*General procedure for the preparation of benzo[*g*]chromenes*

Mixture of benzaldehyde **1** (1.0 mmol), malononitrile **2** (1.0 mmol), 2-hydroxy-1,4-naphthoquinone **3** (1.0 mmol), acetonitrile (3 mL) was stirred thoroughly in the presence of a catalytic amount of nano-NiO (30 mg) at room temperature to afford the corresponding benzo[*g*]chromenes in excellent yields. The progress of the reaction was monitored by TLC. After completion of the reaction, the solid catalyst was filtered from the soluble products and washed with hot EtOH. After cooling, the crude products were precipitated. Pure benzo[*g*]chromenes were obtained in high yields without any further purification.

Spectral characterization of synthesized benzo[g]chromenes**2-Amino-5,10-dioxo-4-phenyl-5,10-dihydro-4H-benzo[g]chromene-3-carbonitrile (3a)**

Orange powder, (94% yield). Melting Point: 263-265 °C (Lit. 260-261 °C); FT-IR (KBr) ($\nu_{\max}/\text{cm}^{-1}$): 3410, 3294, 3187, 2192, 1667, 1594, 1410. ^1H NMR (300 MHz, DMSO- d_6 , δ_{H} (ppm) 4.75 (1H, s, CH), 7.25-7.80 (11H, m, aromatic), 6.43 (2H, s, NH₂). Elemental analysis: Calculated (%) for C₂₀H₁₄N₂O₃ (330.34): C, 72.72; H, 4.27; N, 8.48. Found: C, 72.78; H, 4.24; N, 8.46.

2-Amino-4-(4-chlorophenyl)-5,10-dioxo-5,10-dihydro-4H-benzo[g]chromene-3-carbonitrile (3b)

Orange powder (92% yield). Melting Point: 252-254 °C (Lit. 249-252 °C); FT-IR (KBr) ($\nu_{\max}/\text{cm}^{-1}$): 3412, 3324, 3212, 2194, 1665, 1592, 1418. ^1H NMR (300 MHz, DMSO- d_6): δ_{H} (ppm) 4.61 (1H, s, CH), 7.33-8.07 (10H, m, aromatic) and 6.36 (2H, s, NH₂). Elemental analysis: Calculated (%) for C₂₀H₁₁ClN₂O₃ (362.77): C, 66.22; H, 3.06; N, 7.72. Found: C, 66.34; H, 3.08; N, 7.66.

2-Amino-4-(4-bromophenyl)-5,10-dioxo-5,10-dihydro-4H-benzo[g]chromene-3-carbonitrile (3c)

Orange powder, (91% yield). Melting Point: 251-253 °C (Lit. 252-253 °C); FT-IR (KBr) ($\nu_{\max}/\text{cm}^{-1}$): 3411, 3328, 3192, 2195, 1662, 1593, 1364. ^1H NMR (300 MHz, DMSO- d_6): δ_{H} (ppm) 4.64 (1H, s, CH), 7.26-8.13 (10H, m, aromatic), 6.38 (2H, s, NH₂). Elemental analysis: Calculated (%) for C₂₀H₁₁BrN₂O₃ (407.22): C, 58.99; H, 2.72; N, 6.88. Found: C, 58.87; H, 2.81; N, 6.86.

2-amino-4-(4-hydroxyphenyl)-5,10-dioxo-5,10-dihydro-4H-benzo[g]chromene-3-carbonitrile (3d)

Orange powder (93% yield). Melting Point: 255-257 °C (Lit. 257-258 °C); FT-IR (KBr) ($\nu_{\max}/\text{cm}^{-1}$): 3399, 3327, 3188, 2202, 1668, 1596, 1509. ^1H NMR (300 MHz, DMSO- d_6): δ_{H} (ppm) 4.50 (1H, s, CH), 6.72-8.07 (10H, m, aromatic and NH₂), 9.33 (1H, s, OH). Elemental analysis: Calculated (%) for C₂₀H₁₂N₂O₄ (344.32): C, 69.76; H, 3.51; N, 8.14. Found: C, 69.70; H, 3.56; N, 8.12.

2-Amino-4-(4-nitrophenyl)-5,10-dioxo-5,10-dihydro-4H-benzo[g]chromene-3-carbonitrile (3e)

Orange powder, (94% yield). Melting Point: 233-235 °C (Lit. 233-234 °C); FT-IR (KBr) ($\nu_{\max}/\text{cm}^{-1}$): 3450, 3400, 3345, 2187, 1660, 1600, 1506. ^1H NMR (300 MHz, DMSO- d_6): δ_{H} (ppm) 4.67 (1H, s, CH), 7.41-8.18 (10H, m, aromatic), 6.58 (2H, s, NH₂). Elemental analysis: Calculated (%) for C₂₀H₁₁N₃O₅(373.32): C, 64.35; H, 2.97; N, 11.26. Found: C, 64.41; H, 2.92; N, 11.21.

2-Amino-4-(4-methoxyphenyl)-5,10-dioxo-5,10-dihydro-4H-benzo[g]chromene-3-carbonitrile (3f)

Orange powder, (92% yield). Melting Point: 246-248 °C (Lit. 247-248 °C); FT-IR (KBr) ($\nu_{\max}/\text{cm}^{-1}$): 3445, 3388, 2212, 1745, 1663, 1586, 1457, 1329. ^1H NMR (300 MHz, DMSO- d_6): δ_{H} (ppm) 3.71 (3H, s, OCH₃), 4.57 (1H, s, CH), 6.85-8.05 (10H, m, aromatic and NH₂). Elemental analysis: Calculated (%) for C₂₁H₁₄N₂O₄ (358.35): C, 70.39; H, 3.94; N, 7.82. Found: C, 70.12; H, 3.96; N, 7.84.

2-Amino-4-(2-chlorophenyl)-5,10-dioxo-5,10-dihydro-4H-benzo[g]chromene-3-carbonitrile (3g)

Orange powder (89% yield). Melting Point: 235-237 °C (Lit. 235-237 °C); FT-IR (KBr) ($\nu_{\max}/\text{cm}^{-1}$): 3435, 3310, 3214, 2197, 1650, 1632, 1601. $^1\text{H NMR}$ (400 MHz, DMSO- d_6): δ_{H} (ppm) 5.25 (1H, s, CH), 7.26-8.07 (10H, m, aromatic), 6.32 (2H, s, NH₂). Elemental analysis: Calculated (%) for C₂₀H₁₁ClN₂O₃ (362.77): C, 66.22; H, 3.06; N, 7.72. Found: C, 66.12; H, 3.16; N, 7.74.

2-Amino-4-(2-nitrophenyl)-5,10-dioxo-5,10-dihydro-4H-benzo[g]chromene-3-carbonitrile (3h)

Orange powder (87% yield). Melting Point: 242-244 °C (Lit. 241-243 °C); FT-IR (KBr) ($\nu_{\max}/\text{cm}^{-1}$): 3428, 3316, 3021, 2192, 1662, 1632, 1596. $^1\text{H NMR}$ (400 MHz, DMSO- d_6): δ_{H} (ppm) 4.86 (1H, s, CH), 7.35-8.21 (10H, m, aromatic), 6.41 (2H, s, NH₂). Elemental analysis: Calculated (%) for C₂₀H₁₁N₃O₅ (373.32): C, 64.35; H, 2.97; N, 11.26. Found: C, 64.39; H, 2.99; N, 11.21.

2-Amino-4-(3-methoxyphenyl)-5,10-dioxo-5,10-dihydro-4H-benzo[g]chromene-3-carbonitrile (3i)

Orange powder (88% yield). Melting Point: 248-250 °C (Lit. 249-251 °C); FT-IR (KBr) ($\nu_{\max}/\text{cm}^{-1}$): 3462, 3320, 2933, 2832, 2189, 1677, 1598, 1037,864. $^1\text{H NMR}$ (400 MHz, DMSO- d_6): δ_{H} (ppm) 3.86 (3H, s, OCH₃), 4.57 (1H, s, CH), 7.18-8.09 (10H, m, aromatic), 6.75 (2H, s, NH₂). Elemental analysis: Calculated (%) for C₂₁H₁₄N₂O₄ (358.35): C, 70.39; H, 3.94; N, 7.82. Found: C, 70.29; H, 3.96; N, 7.84.

2-Amino-4-(3,4-dimethoxyphenyl)-5,10-dioxo-5,10-dihydro-4H-benzo[g]chromene-3-carbonitrile (3j)

Orange powder (89% yield). Melting Point: 271-273 °C (Lit. 272-273 °C); FT-IR (KBr) ($\nu_{\max}/\text{cm}^{-1}$): 3388, 3324, 3216, 2946, 2196, 1656, 1601, 1462, 1214, 1132, 1024. $^1\text{H NMR}$ (400 MHz, DMSO- d_6): δ_{H} (ppm) 3.84 (6H, d, OCH₃), 4.68 (1H, s, CH), 7.04-8.05 (10H, m, aromatic), 6.85 (2H, s, NH₂). Elemental analysis: Calculated (%) for C₂₂H₁₆N₂O₅ (388.37): C, 68.04; H, 4.15; N, 7.21. Found: C, 68.14; H, 4.11; N, 7.32.

2-Amino-4-(furan-2-yl)-5,10-dioxo-5,10-dihydro-4H-benzo[g]chromene-3-carbonitrile (3k)

Blackish solid (84% yield). Melting Point: 267-269 °C (Lit. 266-268 °C); FT-IR (KBr) ($\nu_{\max}/\text{cm}^{-1}$): 3418, 3210, 3089, 2328, 2195, 1660, 1638, 1591, 1517, 1440, 1276, 1050, 787, 726, 664, 579. $^1\text{H NMR}$ (400 MHz, DMSO- d_6): δ_{H} (ppm) 6.12 (1H, s, CH), 7.44-8.34 (10H, m, aromatic), 6.12 (2H, s, NH₂). Elemental analysis: Calculated (%) for C₁₈H₁₀N₂O₄ (318.28): C, 67.92; H, 3.17; N, 8.80. Found: C, 67.95; H, 3.14; N, 8.78.

Antibacterial activity

Antibacterial activity was determined by Kirby-Bauer method. The investigated microorganisms were *E.coli*, *Klebsiella*, *Pseudomonas aeruginosa*, *Proteus mirabilis*, *Staphylococcus aureus*, *Staphylococcus saprophytic* and *Candida albicans*. Initially, a suspension of medium was prepared and sterilized as direct by the manufacturer. The medium was poured into Petri dishes to a depth of 4 mm and stored at +4 °C and the pH of the medium should be 7.2 to 7.4. Plates were inoculated within 15 min of preparation of the suspension. A sterile cotton-wool swab dipped into the suspension and inoculated over the entire surface of the plate in three directions. After the inoculums had dried, single discs were

applied with forceps and pressed gently to ensure even contact with the medium. The disc was stocked in standard drugs (Ciprofloxacin and Flucanazole) and test solutions separately and then place on inoculated culture medium. Discs should be stored at +4 °C in sealed containers with a desiccant and should be allowed to come to room temperature before the containers were opened. Plates were incubated for 16 to 18 hours at 35 to 37 °C aerobically. Bacterial growth inhibition was determined as the diameter of inhibition zones around the disc. The resultant clear zones were measured in millimeters and compared against standard drugs.

Results and Discussion

In continuation of our findings of new catalyst for the synthesis of benzo[g]chromenes using aldehydes **1**, malononitrile **2**, 2-hydroxy-1, 4-naphthoquinone **3** as a model reaction a wide variety of catalyst such as different transition metals salts (Cu, Zn, Fe, Co, Sn, Ni and Cd) were employed at room temperature. The outcome of the products is listed in Table 1. Among the various transition metal salts nickel (Table 1, Entry 6) is found to give the excellent yield at an ambient condition.

Table 1. Synthesis of benzo[g]chromenes using various transition metal salts^a

Entry	Catalyst	Time, h	Yield, % ^b
1	CuCl ₂ .2H ₂ O	8	36
2	ZnCl ₂ .6H ₂ O	8	48
3	FeCl ₃ .6H ₂ O	8	29
4	CoCl ₂ .6H ₂ O	8	52
5	SnCl ₂ .2H ₂ O	8	26
6	NiCl ₂ .6H ₂ O	8	78
7	CdCl ₂ .2H ₂ O	8	34
8	-	24	Nil

^aBenzaldehyde (1mmol), malononitrile (1 mmol), 2-hydroxy-1,4-naphthoquinone (1 mmol), catalyst 200 mg, ACN, room temperature, ^bIsolated yield

These results made to choose nickel salts as a precursor for metal oxide nanoparticles. When particle size is reduced to nano dimensions, the consulting atoms have highly defective coordination environments. Most of the atoms locate at the surface and have unsatisfied valencies. The catalytic activity of nano-NiO was confirmed when there is no formation of product in the absence of catalyst (Table 1, Entry 8).

The structural and chemical characterizations of nano-NiO were performed by using TEM, SEM-EDX, XRD, FT-IR and UV spectroscopy. The TEM image of nickel oxide shown in Figure 1(a) reveals that most of the prepared nanoparticles are spherical shaped and the size is in the range of 10-15 nm. Scanning Electron microscope (SEM, Figure 1(b)) indicates that the prepared nanoparticles are spherical shape in uniform distribution which is in good agreement with the result of TEM. Energy dispersive spectrum (Figure 1(c)) indicates the presence of Ni and O elements and it confirms the purity of the synthesized nanoparticles. The total nickel content present in NiO is found to be 43.01 atom%.

The crystallite size of nickel oxide nanoparticles is determined by XRD (Figure 2) and it indicates that NiO have diffraction peaks of a face centered cubic crystal lattice at around $2\theta = 37.5, 43.6, 63.1, 75.7$ and 79.7 which are a result of Ni (111), (200), (220), (311) and (222) respectively, (JCPDS-ICDD, card No. 78-0429). The diffraction peak (200) is used to calculate the particle size and it is found to be about 8.46 nm, by using the following Debye Scherrer equation¹⁸ given below:

$$D = K\lambda / \beta \cos\theta \quad (1)$$

Where K = a coefficient (0.89); λ = the wavelength of the x-rays used (1.54056 Å); β = the full width half-maximum of the respective diffraction peak (rad) and θ = the angle at the position of the peak maximum (rad).

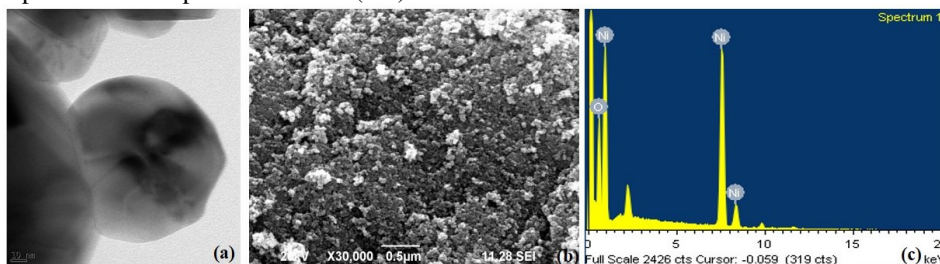


Figure 1. (a) TEM images of nano-NiO (b) SEM image of nano-NiO (c) EDX image of nano-NiO

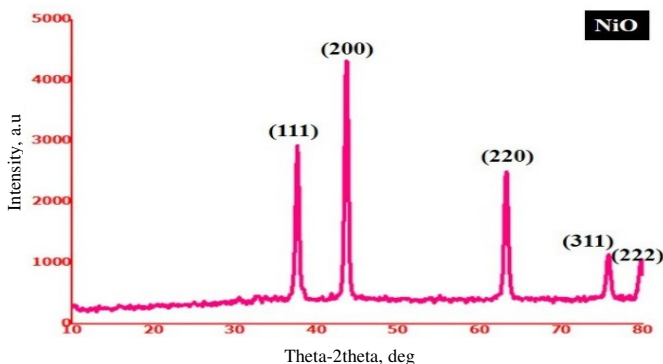


Figure 2. XRD image of nano-NiO

FT-IR spectrum (Figure 3 (i)) shows that the broad absorption band centered at 3457 cm^{-1} is attributable to the O-H stretching vibrations due to the adsorption of water in air when FT-IR sample disks were prepared in an open air. The broad absorption band in the region 447.56 cm^{-1} is assigned to Ni-O stretching vibration mode of the octahedral NiO_6 groups in the face centered cubic NiO structure¹⁹. Since there is no formation of peaks at the region of 1632 cm^{-1} , indicates the absence of Ni-OH bond. It clearly indicates the complete formation of NiO after calcination at $450\text{ }^\circ\text{C}$. The broadness of the absorption band indicates that the NiO powders are nanocrystals and well crystallized.

The strong absorption peak at 359.3 nm indicates the formation of NiO and this strong band is due to the electronic transition from valence band to the conduction band in the NiO semiconductor²⁰. But in case of bulk NiO powder does not show any observable absorption band. By using Tauc²¹ relation we can calculate the optical band gap of NiO nanoparticles from the absorption spectrum.

$$\epsilon h\nu = C(h\nu - E_g)^n \quad (2)$$

Where C is a constant, ϵ is molar extinction coefficient, E_g is the average band gap of the material and n depends on the type of transition. For the prepared NiO sample, the absorption band appears at 359.3 nm is fairly blue shifted from the absorption edge of bulk NiO. The calculated band energy gap from the UV absorption is found to be 3.98 eV which is found to be higher than bulk NiO. So it confirms that the prepared NiO is in nano scale²².

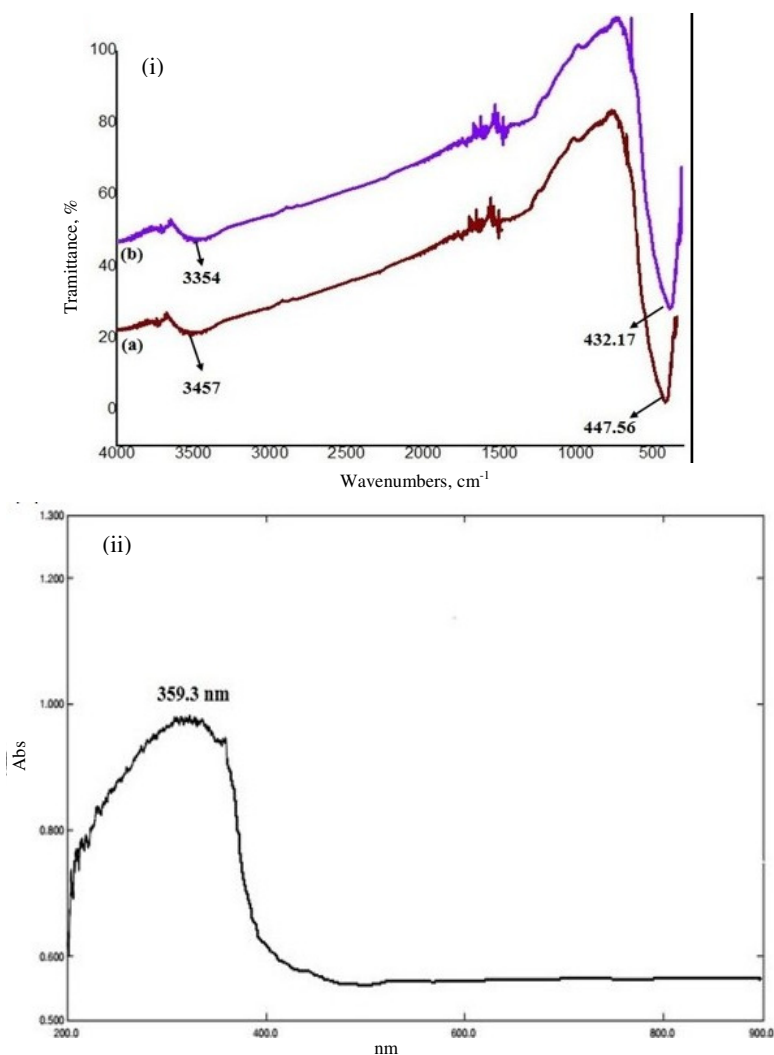
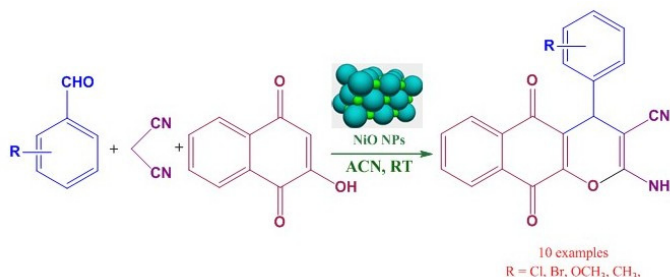


Figure 3. (i) FT-IR spectrum of (a) Nano-NiO (b) Reused nano-NiO (ii) UV-Vis spectrum of nano-NiO

Synthesis of benzo[g]chromenes in the presence of nano-NiO as catalyst

Metal oxides exemplifies a wide class of materials that have been investigated extensively due to their interesting magnetic, electronic and catalytic properties. Recently for many organic transformation reactions nickel oxide nanoparticles have been employed as easily recoverable stable catalyst with simple workup and it prevents the contamination of products. Hence it is used as a safe reusable heterogeneous catalyst. But the catalytic activity of NiO for the synthesis of benzo[g]chromenes is not reported earlier. The synthesis of benzo[g]chromenes using acetonitrile as solvent in the reaction of various aldehyde (1), malononitrile (2) and 2-hydroxy-1,4-naphthoquinone (3) in a one-pot multi-component reaction gives an excellent yield in the presence of nano-NiO as a catalyst (Scheme 1).



Scheme 1. Synthesis of benzo[g]chromene derivatives in the presence of nano-NiO

The model reaction has been optimized by using various solvents, catalyst loading and reaction conditions based on temperature. Initially, the effect of the solvent has been studied on the model reaction as shown in Table 2. The reaction was carried out in the presence of different solvents such as dichloromethane, DMF, acetonitrile, ethanol, methanol, ethyl acetate, chloroform, water and dioxane. Among the various solvents, in presence of acetonitrile we obtain the highest yield (Table 2, Entry 3).

Table 2. Optimization of solvents, catalyst loading and reaction conditions for the synthesis of benzo[g]chromenes^a

Entry	Catalyst	Solvent	Time, h	Yield, % ^b
1	NiO	Dichloromethane	2	59
2	NiO	DMF	2	66
3	NiO	Acetonitrile	0.25	94
4	NiO	Ethanol	2.5	76
5	NiO	Methanol	3	62
6	NiO	Ethyl acetate	4	55
7	NiO	Chloroform	4	78
8	NiO	Water	2.5	82
9	NiO	Dioxane	8	46
10	NiO	-	8	54
11 ^c	NiO	Acetonitrile	0.25	64, 75, 94, 96
12 ^d	NiO	Acetonitrile	0.25	82, 94, 95
13 ^e	NiO	Acetonitrile	0.25	94, 61

^aBenzaldehyde (1 mmol), malononitrile (1 mmol), 2-hydroxy-1,4-naphthoquinone (1 mmol), catalyst 30 mg, ACN 3 mL, room temperature ^bIsolated yield ^cReaction carried out with different catalyst loading such as 10 mg, 20 mg, 30 mg and 40 mg ^dDifferent solvent ratio (1 mL, 3 mL, 5mL) respectively. ^eReaction carried out at different temperature (RT, reflux)

Catalyst loading is another important parameter for the reaction efficiency. Four sets of model reaction were carried out with different catalyst loading to obtain the excellent yield. In absence of catalyst there is no formation of products. While adding 10 and 20 mg of nano-NiO, the yield of the product is in desirable range (Table 2, Entry 11). While increasing the amount of catalyst to 30 mg, there is an increase in yield to 94%. Further increase in catalyst does not affect the yield in greater extent. Hence the optimum catalyst loading is found to be 30 mg.

After optimizing solvent and catalyst loading, the amount of solvent and the temperature effect were studied in the model reaction. It is observed that 3 mL solvent (Acetonitrile) is optimum for better reaction yield (Table 2, Entry 12). Similarly room temperature

is more sufficient to obtain the good yield within a short reaction time (Table 2, Entry 13). The optimized reaction conditions for an excellent yield of the model reaction without any byproduct formation is 30 mg nano-NiO, 3 mL Acetonitrile solvent at room temperature.

Table 3. One-pot synthesis of substituted 2-amino-4*H*-benzo[*g*]chromenes using nano-NiO as catalyst under optimum reaction conditions^a

Entry	R	Product	Time, min	Yield, % ^b	Melting point, °C
1 ^c	C ₆ H ₅	3a	15	94, 96 ^c	263-265 ²³
2	4-ClC ₆ H ₄	3b	20	92	252-254 ¹⁰
3	4-BrC ₆ H ₄	3c	15	91	251-253 ²³
4	4-OHC ₆ H ₄	3d	22	93	255-257 ¹⁰
5	4-NO ₂ C ₆ H ₄	3e	14	94	233-235 ²³
6	4-CH ₃ OC ₆ H ₄	3f	15	92	246-248 ¹⁰
7	2-ClC ₆ H ₄	3g	20	89	235-237 ²³
8	2-NO ₂ C ₆ H ₄	3h	17	87	242-244 ²³
9	3-CH ₃ OC ₆ H ₄	3i	24	88	248-250 ²³
10	3,4-CH ₃ OC ₆ H ₃	3j	20	94	271-273 ²³
11	2-furfuryl	3k	30	84	267-269 ¹⁵
12	CH ₃ CHO	3l	12 h	-	-
13	CH ₃ CH ₂ CHO	3m	12 h	-	-
14	<i>n</i> -Heptanal	3n	12 h	-	-
15	C ₆ H ₅ CH=CHCHO	3o	12 h	-	-

^aBenzaldehyde (1 mmol), malononitrile (1 mmol), 2-hydroxy-1,4-naphthoquinone (1 mmol), catalyst 30 mg, ACN 3 mL, room temperature ^bIsolated yield ^cYield of gram scale reaction with Benzaldehyde (10 mmol), malononitrile (10 mmol), 2-hydroxy-1,4-naphthoquinone (10 mmol)

Under these optimized conditions, the scope and the efficiency of the reaction were explored for the synthesis of a wide variety of substituted 2-amino-4*H*-benzo[*g*]chromenes with divergent aldehydes including aromatic, heteroaromatic, aliphatic aldehydes were reported in Table 3. Those bearing electron donating or electron withdrawing group at ortho, para or meta positions in the benzene ring gives the desired product in good to excellent yield (Table 3, Entry 1-10) and they led to the formation of the corresponding highly functionalized benzo[*g*]chromene derivatives (**3a-3k**) at ambient condition without any desirable byproduct. It is noteworthy that this methodology worked well even for spatially-hindered aldehydes (Table 3, Entry 7-10). In case of aliphatic aldehydes such as acetaldehyde, propionaldehyde, *n*-heptanal, cinnamaldehyde carried out in model reaction gives no such desired products even after a long reaction time (Table 3, Entry 12- 15). All the highly functionalized benzo[*g*]chromene derivatives were isolated and recrystallized from ethanol; no column chromatographic technique is required for purification. The isolated products were characterized on the basis of analytical and spectral studies including melting point, FT-IR, proton NMR and elemental analyses. The model reaction was carried out on a larger scale and the similar outcome was achieved (Table 3, Entry 1^c). This establishes the efficiency of catalyst for industrial production.

Finally, the reusability of catalyst (Figure 4) was investigated by isolating the catalyst from the reaction medium and washed with acetone, dried and reused again for the same model reaction. It was found that it can afford a good yield even after five consecutive runs. It is also confirmed by FT-IR spectrum of fresh and the recovered catalyst after 5th run (Figure 3(i)). The shape, position and relative intensity of all characteristic peaks are well preserved. This proves that there is no change on the chemical structure.

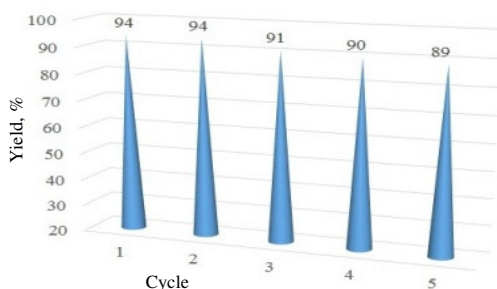


Figure 4. Reusability performance of nano-NiO in the model reaction

On the basis of the above results and also in accordance with earlier literature reports¹⁰, a plausible reaction pathway is proposed as shown in Figure 5. Nano-NiO facilitates the Knoevenagel condensation reaction between an aldehyde **1** and malononitrile **2**; through Lewis acid sites (Ni^{2+}) coordinated to the oxygen of the carbonyl groups²⁴. On the other hand, nano-NiO can activate methylene compounds so that deprotonation of the C-H bond occurs in the presence of Lewis basic sites (O^{2-}) and lead to the formation of arylidenemalononitrile **4** which contains an electron-poor C=C double bond, then the obtained intermediate **4** has been attacked by the 2-hydroxy-1, 4-naphthoquinone **3**, which leads to the intermediate **5**. Such an addition intermediate may contribute in a cyclization reaction to generate **6**; which may undergo tautomerization to produce the fused heterocyclic systems.

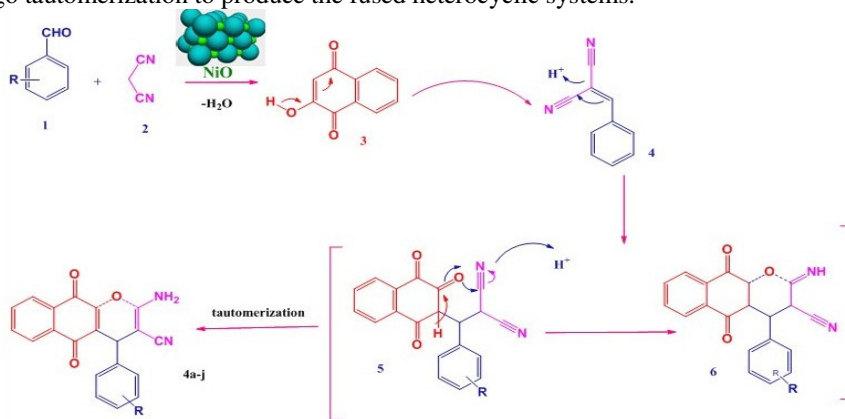


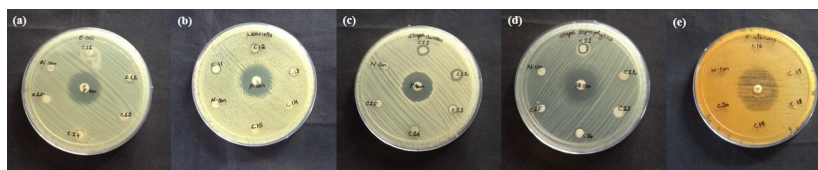
Figure 5. Plausible mechanism for the formation of benzo[g]chromenes using nano-NiO

Antibacterial activity

The zones of inhibition are measured by using disc diffusion method (Figure 6 & Table 4). The antibacterial and antifungal studies reveals that all the fused benzo[g]chromene derivatives showed significant anti-microbial activity on comparing with the standard drug of ciprofloxacin for gram positive and gram negative bacteria, Flucanazole for fungi. Compounds containing nitro, chloro group showed greater activity compared with compounds containing hydroxyl, methoxy group which exhibits mild to moderate activity. Hence this study reveals that the substituent in the benzene ring changes the antibacterial activity. Electron withdrawing group in the benzene ring exhibits more potent towards the microorganisms than the electron donating group present in the benzene ring. In case of fungal activity, only few compounds exhibit significant antifungal inhibition.

Table 4. Zone of inhibition for synthesized benzo[g]chromene derivatives against microorganisms

Compounds	Zone of inhibition, mm						
	Gram (+) and Gram (-) bacteria						Fungi
	<i>E.coli</i>	<i>K. pneumonia</i>	<i>P.aeruginosa</i>	<i>Proteus mirabilis</i>	<i>S.aureus</i>	<i>S.saprophyticus</i>	<i>Candida albicans</i>
3a	11	13	9	9	10	10	14
3b	14	15	9	8	12	9	-
3c	-	9	-	11	14	10	11
3d	10	-	-	13	8	-	-
3e	8	11	11	10	11	12	10
3f	8	9	12	-	-	-	14
3g	11	14	14	12	13	15	13
3h	13	18	10	9	14	11	-
3i	9	11	-	7	-	10	-
3j	12	14	5	11	15	14	-
3k	7	-	-	10	10	11	-
Control	20	22	18	17	21	20	29
Standard Drugs	Ciprofloxacin			Flucanazole			

**Figure 6.** Zone of inhibition of certain microorganisms of synthesized benzo[g]chromenes [a) *E.coli*, b) *K. pneumonia*, c) *S. aureus*, d) *S.saprophyticus* and e) *Candida albicans*]

Conclusion

Nano-NiO acts as an environmental friendly solid heterogeneous catalyst in the one-pot atom economical reaction for the synthesis of functionalized benzo[g]chromenes derivatives from various aromatic, heteroaromatic aldehydes, malonitrile and 2-hydroxy-1,4-naphthoquinone via Knoevenagel cyclocondensation reaction in presence of acetonitrile as solvent. The highlights of the present procedure are easy workup, good functional groups tolerance, high yields, shorter reaction times, ambient temperature, easy isolation of products, high life span for catalyst and low catalyst loading due to larger active sites. Synthesized compounds underwent Kirby-Bauer test and exhibit mild to moderate activity against selected gram (+) and gram (-) bacteria depending on the substituent's in the aromatic ring.

References

1. Ough M, Lewis A, Bey E A, Gao J, Ritchie J M, Bornmann W, Oberley L W and Cullen J J, *Canc Biol Ther.*, 2005, **4(1)**, 102-109; DOI:10.4161/cbt.4.1.1382
2. Moon D O, Choi Y H, Kim N D, Park Y M and Kim G Y, *Int Immunopharmacol.*, 2007, **7(4)**, 506-514; DOI:10.1016/j.intimp.2006.12.006
3. Shestopalov A M, Emelianova Y M and Nesterov V N, *Russ Chem Bull.*, 2003, **52(5)**, 1164-1172.

4. Elinson M N, Dorofeev A S, Feducovich S K, Gorbunov S V, Nasybullin R F and Stepanov N O, *Tetrahedron Lett.*, 2006, **47(43)**, 7629-7633; DOI:10.1016/j.tetlet.2006.08.053
5. Sun W, Cama L J, Birzin E T, Warriar S, Locco L, Mosley R, Hammond M L and Rohrer S P, *Bioorg Med Chem Lett.*, 2006, **16(6)**, 1468-1472; DOI:10.1016/j.bmcl.2005.12.057
6. Stachulski A. V, Berry N G, Low A C L, Moores S L, Row E, Warhurst D C, Adagu I S and Rossignol J F, *J Med Chem.*, 2006, **49(4)**, 1450-1454; DOI:10.1021/jm050973f
7. Hunger K, *Industrial Dyes*. Weinheim: WILEY-VCH Verlag, 2003.
8. Gold H, In: Venkataraman H, Ed., *The Chemistry of Synthetic Dyes*. New York: Academic Press, 1971.
9. Yao C S, Yu C X, Li T J and Tu S J, *Chin J Chem.*, 2009, **27**, 1989-1994; DOI: 10.1002/cjoc.200990334
10. Shaabani A. Ghadari R, Ghasemi S, Pedarpour M, Rezayan A H, Sarvary A and Ng S W, *J Comb Chem.*, 2009, **11(6)**, 956-959; DOI:10.1021/cc900101w
11. Khurana J M, Nand B and Saluja P, *Tetrahedron*, 2010, **66(30)**, 5637-5641; DOI:10.1016/j.tet.2010.05.082
12. Shaterian H R and Kangani K, *Sci Iran.*, 2013, **20(3)**, 571-579; DOI:10.1016/j.scient.2012.11.019
13. Maleki B, Babae S and Tayeb R, *Appl Organomet Chem.*, 2015, **29(6)**, 408-411; DOI:10.1002/aoc.3306
14. Dekamin M G, Eslami M and Maleki A, *Tetrahedron*, 2013, **69(3)**, 1074-1085; DOI:10.1016/j.tet.2012.11.068
15. Brahmachari G and Banerjee B, *ACS Sustainable Chem Eng.*, 2014, **2(3)**, 411-422; DOI:10.1021/sc400312n
16. Maleki B, *Org Prepar Proc Int.*, 2016, **48(1)**, 81-87; DOI:10.1080/00304948.2016.1127104
17. Lu I, Ruiz Aranzaes J and Astruc D, *Angewandte Chemie*, 2005, **44(45)**, 7399-7404; DOI:10.1002/anie.200502848
18. Kotal A, Paira T K, Banerjee S and Mandal T K, *Langmuir*, 2010, **26(9)**, 6576-6582; DOI:10.1021/la903923q
19. Warad I, Hammouti B, Hadda T B, Boshala A and Haddad S F, *Res Chem Intermed.* 2013, **39(9)**, 4011-4020.
20. Salavati Niasari M, Mohandes F, Davar F, Mazaheri M, Monemzadeh M and Yavarinia N, *Inorg Chim Acta*, 2009, **362(10)**, 3691-3697; DOI:10.1016/j.ica.2009.04.025
21. Tauc J, *Mater Res Bull.*, 1968, **3**, 37-46.
22. Makhlof S A, Parker F T, Spada F E and Berkowitz A E, *J Appl Phys.*, 1997, **81(8)**, 5561-5563; DOI:10.1063/1.364661
23. Shaterian H R and Mohammadnia M, *J Mol Liq.*, 2013, **177**, 353-360; DOI:10.1016/j.molliq.2012.10.012
24. Sheldon R A and Downing R S, *Appl Cataly A*, 1999, **189(2)**, 163-183; DOI:10.1016/S0926-860X(99)00274-4